

# The effect of baryon-CDM relative velocity and density perturbations on the clustering of galaxies

Fabian Schmidt

Max-Planck-Institut für Astrophysik, Karl-Schwarzschild-Str. 1, 85748 Garching, Germany  
(Dated: June 26, 2022)

Pre-recombination acoustic oscillations induce non-adiabatic perturbations between baryons and dark matter, corresponding to a constant relative-density  $\delta_{bc}$  and decaying relative-velocity perturbation  $v_{bc}$ . Due to their significant large-scale correlations and prominent baryon acoustic oscillation (BAO) features, these modes are potentially important for the use of the BAO as standard ruler. We present a complete treatment of the effects of the baryon-CDM perturbations on galaxy clustering in the context of a rigorous perturbative bias expansion. The leading effects are proportional to  $\delta_{bc}$  and  $\theta_{bc} = \partial_t v_{bc}^i$ . We estimate the magnitude of these terms through the excursion set approach. The contribution from  $v_{bc}^2$ , which has attracted significant attention recently, contributes at subleading (1-loop) order. Depending on its bias parameter, which is highly uncertain, it could be smaller, comparable to, or up to an order of magnitude larger than the leading  $\theta_{bc}$  term. On the other hand,  $\delta_{bc}$  is expected to be by far the largest contribution, and the most significant potential worry for the BAO ruler. We also give complete expressions of the galaxy power spectrum at 1-loop order, identifying several new terms.

## I. INTRODUCTION

Our Universe contains two dominant matter components: cold dark matter (CDM,  $c$ ) and baryons ( $b$ , i.e. all non-relativistic standard model particles). In studies of structure formation, we commonly treat these two fluids as a single, comoving matter fluid (or, a collection of collisionless particles). However, the coupling of baryons to radiation in the primordial plasma before recombination leads to relative perturbations in density and velocity of the baryon and CDM components. While significant initially, these perturbations grow less rapidly than the adiabatic growing mode and hence are very small in the low-redshift universe. However, since these perturbations have significant large-scale correlations, they are potentially detectable through their imprint in the clustering of galaxies on large scales. Moreover, they retain a significantly stronger imprint of the BAO feature than the adiabatic growing mode, so that they are of relevance for the use of the BAO feature in the galaxy two-point function as a standard ruler [1, 2].

Let us consider the evolution of baryons and CDM after baryon-photon decoupling, approximating both as pressureless fluids, which is appropriate on sufficiently large scales. The evolution of two such fluids coupled by gravity is described by the Euler and continuity equations which at linear order become

$$\begin{aligned} \frac{\partial}{\partial \tau} \delta_s &= -\theta_s, \quad s \in \{b, c\} \\ \frac{\partial}{\partial \tau} \theta_s + \mathcal{H} \theta_s &= -\frac{3}{2} \Omega_m(a) \mathcal{H}^2 \delta_m, \end{aligned} \quad (1)$$

where  $\delta_s \equiv \delta \rho_s / \bar{\rho}_s$ ,  $\theta_s = \partial_j v_s^j$ , while  $\delta_m = f_b \delta_b + (1 - f_b) \delta_c$  is the total matter density perturbation and  $f_b = \Omega_b / \Omega_m$ . It is useful to combine these equations and to rewrite

them in terms of  $\delta_m$  and  $\delta_r = \delta_b - \delta_c$ :

$$\begin{aligned} \frac{\partial^2}{\partial \tau^2} \delta_m + \mathcal{H} \frac{\partial}{\partial \tau} \delta_m - \frac{3}{2} \Omega_m(a) \mathcal{H}^2 \delta_m &= 0 \\ \frac{\partial^2}{\partial \tau^2} \delta_r + \mathcal{H} \frac{\partial}{\partial \tau} \delta_r &= 0. \end{aligned} \quad (2)$$

We now immediately obtain the general solution of these two decoupled ODE as

$$\begin{aligned} \delta_m(\tau) &= A_+ D_+(\tau) + A_- H(\tau) \\ \delta_r(\tau) &= R_+ + R_- D_r(\tau), \end{aligned} \quad (3)$$

where  $A_{\pm}$ ,  $R_{\pm}$  are constants and

$$D_r(\tau) \equiv H_0^{-1} \int_{\tau}^{\infty} \frac{d\tau'}{a(\tau')} = \int_{\ln a(\tau)}^{\infty} \frac{d \ln a'}{a'^2 H(a') / H_0}. \quad (4)$$

During matter domination, this approaches the Einstein-de Sitter result  $D_r = -2a^{-1/2}$ .  $\delta_m$  contains the two well-known growing and decaying modes  $\propto A_{\pm}$  of adiabatic perturbations. A third mode  $\propto R_+ \equiv \delta_{bc}$  is a constant compensated perturbation  $\delta \rho_c = -\delta \rho_b$ , corresponding to  $\delta_m = 0$  while  $\delta_r \neq 0$  [3–5]. This mode can be seen as modulating the local baryon-CDM ratio,  $f_{b,\text{loc}} = f_b(1 + \delta_{bc})$ . The significance of the fourth decaying mode  $\propto R_-$  becomes clear by considering

$$\frac{\theta_{bc}}{aH} \equiv \frac{\theta_b - \theta_c}{aH} = R_- \frac{H_0}{a^2 H(a)}, \quad R_- = \frac{\theta_{bc,0}}{H_0}, \quad (5)$$

where  $\theta_{bc,0} \equiv \theta_{bc}(z=0)$ . Thus, this mode corresponds to an initial relative velocity  $v_{bc} \propto 1/a$  between the two fluids.

With few exceptions [6–8, 34], studies of structure formation using perturbation theory and N-body simulations have focused on the adiabatic growing mode  $A_+$ . Ref. [9] pointed out that pre-recombination plasma waves (baryon acoustic oscillations, BAO) lead to a significant

streaming velocity  $\mathbf{v}_{bc}$  at the epoch of baryon-photon decoupling  $\tau_{\text{dec}}$ . This can leave an imprint in low-redshift structure which assembled out of low-mass halos at high redshifts [10–14]. Similarly, the  $R_+$ -mode is also sourced during recombination [3]. Both  $R_-$  and  $R_+$  have significant large-scale correlations and in particular large BAO features (Fig. 3). For simplicity, we will refer to  $R_{\pm}$  jointly as *baryon-CDM perturbations* in the following.

Since galaxy formation depends sensitively on both baryons and CDM, it is crucial to include these modes when making predictions for galaxy clustering.<sup>1</sup> The goal of this paper is to provide a recipe for a complete description of these effects within a rigorous perturbation theory approach (renormalized bias expansion [15–17], which can be seen as an effective field theory [18, 19]). As an example, we derive the galaxy auto and cross power spectra including the leading (1-loop) nonlinear correction. Moreover, we provide quantitative estimates of the bias parameters that control the magnitude of the baryon-CDM effects on galaxy clustering.

Previously, of the relative density perturbations only a perfectly uniform streaming velocity  $\mathbf{v}_{bc}$  has been considered in detail, that is  $\theta_{bc}$  was set to zero (but see [20]).  $\mathbf{v}_{bc}$  itself can only enter at second order in the galaxy density, since it is a vector, so that the leading contribution to the galaxy density perturbation is [10–14]

$$\delta_g(\mathbf{x}, \tau) \supset b_{v^2}^{bc}(\tau) [\mathbf{v}_{bc}^2 - \sigma_{v_{bc}}^2(\tau)]. \quad (6)$$

In order to assess the quantitative impact of the term in Eq. (6), we need an estimate for the bias parameter  $b_{v^2}^{bc}$ . Ref. [10] argued that  $\mathbf{v}_{bc}$  increases the effective sound speed  $c_s$  of the neutral gas, so that the Jeans mass  $M_J$  increases by a factor  $[1 + v_{bc}^2/c_s^2]^{3/2}$ . This leads to large effects on low-mass halos prior to reionization, as investigated using small-box simulations in [21–23]. However, how these are transferred to the number density of galaxies at low redshifts is unclear.  $b_{v^2}^{bc}$  could be as small as  $\sim 10^{-5} \sigma_{v_{bc}}^{-2}$  [14, 21]. The fiducial value adopted in previous studies is [10–12, 14],

$$b_{v^2}^{bc} \sim 0.01 \sigma_{v_{bc}}^{-2}(z) \approx 9.2 \times 10^{11} (1+z)^{-2}. \quad (7)$$

at redshifts  $z \lesssim 2$ . Note that given the non-detection in current data,  $b_{v^2}^{bc}$  cannot be much larger than this [12]. While Eq. (6) can only contribute to the galaxy power spectrum at 1-loop order, the quantities  $\delta_{bc}$ ,  $\theta_{bc}$  discussed above, corresponding to the modes  $R_+$ ,  $R_-$ , respectively, enter at linear order, and are thus the leading effects unless their bias parameters are highly suppressed compared to  $b_{v^2}$ .

So far, we have neglected radiation and anisotropic stress, which is sufficiently accurate at  $z \lesssim 20$  but not at

higher redshifts. While not important for the formation of structure, this approximation becomes important if one uses transfer function outputs from Boltzmann codes at higher redshifts. Instead, one should match the modes  $A_+$ ,  $R_{\pm}$  from the transfer function output at low redshift. We discuss this in App. A.

The outline of the paper is as follows. We begin with the leading, linear galaxy power spectrum on large scales in Sec. II, and present several estimates for the bias parameters  $b_{\theta}^{bc}$ ,  $b_{\delta}^{bc}$  appearing at this order. In Sec. III, we show how a general bias expansion can be constructed up to any desired order. We also give the complete expressions for the galaxy-auto and cross power spectra at 1-loop order, performing a renormalization of the bias parameters in the process. We conclude in Sec. IV. In the appendix, we discuss how to obtain the transfer functions for  $\delta_{bc}$ ,  $\mathbf{v}_{bc}$ , and provide some details on the spherical collapse calculation used.

Throughout we set  $c = 1$ , and, for numerical results, assume a flat  $\Lambda$ CDM cosmology with  $\Omega_m = 0.27$ ,  $h = 0.7$ ,  $\Omega_b h^2 = 0.023$ ,  $n_s = 0.95$ ,  $\sigma_8 = 0.791$ , and transfer functions given by CAMB [24] (see App. A). This yields for the RMS streaming velocity  $\sigma_{v_{bc}}(z) \equiv \langle \mathbf{v}_{bc}^2 \rangle^{1/2} = 0.031(1+z)$  km/s.

## II. GALAXY CLUSTERING AND BARYON-CDM PERTURBATIONS: LINEAR ORDER

Our goal is to write the galaxy density perturbation as

$$\delta_g(\mathbf{x}, \tau) \equiv \frac{n_g}{\bar{n}_g} - 1 = \sum_O b_O(\tau) O(\mathbf{x}, \tau), \quad (8)$$

where  $b_O(\tau)$  are bias parameters while  $O(\mathbf{x}, \tau)$  denote operators (statistical fields). Since the galaxy density is a (3-)scalar, the  $O$  also have to be scalar operators. Moreover, we classify terms in the expansion in Eq. (8) by the order in perturbation theory of each operator.

It is clear from our discussion in Sec. I that, at linear order, we have to allow for  $\delta_g$  to depend on all modes of the baryon-CDM fluid system. This results in three terms:

$$\begin{aligned} \delta_g^{(1)}(\mathbf{x}, \tau) &= b_1 \delta_m^{(1)}(\mathbf{x}, \tau) + b_{R_+}(\tau) R_+(\mathbf{q}[\mathbf{x}, \tau], \tau) \\ &\quad + b_{R_-}(\tau) R_-(\mathbf{q}[\mathbf{x}, \tau], \tau) \\ &= b_1 \delta_m^{(1)}(\mathbf{x}, \tau) + b_{\theta}^{bc} \theta_{bc}(\mathbf{q}, \tau) + b_{\delta}^{bc} \delta_{bc}(\mathbf{q}), \end{aligned} \quad (9)$$

where in the second line we have used Eq. (5) and defined  $\delta_{bc} \equiv R_+$  [whereas  $\delta_r$  receives contributions from both  $\delta_{bc}$  and  $\theta_{bc}$ , Eq. (3)]. Note that  $R_{\pm}$ ,  $\theta_{bc}$ ,  $\delta_{bc}$  [as well as  $\mathbf{v}_{bc}$  in Eq. (6)] are to be evaluated at the Lagrangian position  $\mathbf{q}[\mathbf{x}, \tau]$  corresponding to  $(\mathbf{x}, \tau)$  [14].<sup>2</sup> At linear

<sup>1</sup> Throughout this paper, we ignore the decaying mode  $A_-$ , since it is not sourced significantly by recombination physics and decays very rapidly.

<sup>2</sup> The precisely correct argument is the position of the fluid at

order we can neglect this distinction, but it will reappear in Sec. III. A quadratic term such as Eq. (6) enters the galaxy two-point function at subleading (1-loop) order, while the terms written in Eq. (9) already appear at leading order. Refs. [3, 5] considered the term  $\delta_{bc}$ , while [14] introduced the term  $\theta_{bc}$ , albeit with a coefficient which we will argue to be unphysical in Sec. II C.

In order to assess the quantitative importance of the new terms in Eq. (9), we need estimates for the bias parameters  $b_\theta^{bc}$ ,  $b_\delta^{bc}$ . In the next sections, we will discuss several such estimates.

### A. Bias estimate 1: local Eulerian biasing

We begin by considering a simple toy model, namely local Eulerian biasing. Let us assume the galaxy density is a simple local function of the CDM and baryon densities  $\rho_c(\mathbf{x}, z)$ ,  $\rho_m(\mathbf{x}, z)$ , smoothed on some small scale that is not relevant for large-scale statistics. We can thus write  $n_g(\mathbf{x}, z) = F_g[\delta_m(\mathbf{x}, z), \delta_r(\mathbf{x}, z)]$ . The linear bias w.r.t  $\delta_m$  is defined as the response of  $n_g$  to a long-wavelength perturbation in the total matter, and in this model is thus given by

$$b_1 = \frac{1}{F_g[0]} \left. \frac{\partial F_g}{\partial \delta_m} \right|_0. \quad (10)$$

Similarly, we define

$$b_r = \frac{1}{F_g[0]} \left. \frac{\partial F_g}{\partial \delta_r} \right|_0, \quad (11)$$

which essentially quantifies the response of the galaxy density to a change in the local baryon-CDM ratio. We then trivially have  $b_\delta^{bc} = b_r$ . Since a change in the local baryon-CDM ratio changes the total baryonic mass available to form stars, we expect  $b_r$  to be of order one for real galaxies. In the remainder of the paper, we will choose  $b_\delta^{bc} = 1$  as fiducial value.

In order to derive  $b_\theta^{bc}$ , we note that a nonzero  $\theta_{bc}(\mathbf{x}, z)$  is associated with a nonzero relative density perturbation derived above, given by Eq. (3),

$$\delta_r \Big|_{\theta_{bc}} = \frac{\theta_{bc,0}}{H_0} D_r(\tau) \approx -2 \frac{\theta_{bc}(z)}{H_0} (1+z)^{-1/2}, \quad (12)$$

where the second relation holds in matter domination. We then have

$$b_\theta^{bc} = \frac{1}{\bar{n}_g} \left. \frac{\partial \bar{n}_g}{\partial \theta_{bc}(z)} \right|_0 = b_r \frac{\partial \delta_r}{\partial \theta_{bc}(z)} = -2(1+z)^{-1/2} H_0^{-1} b_r. \quad (13)$$

Thus, assuming  $b_r$  is of order one,  $b_\theta^{bc}$  is estimated to be of order  $H_0^{-1}$ .

---

$\tau_{\text{dec}}$ . However, this distinction makes a negligible difference, of the same order as other nonlinear terms at recombination not considered here.

### B. Bias estimate 2: excursion set

In order to improve upon this model, we consider the excursion set approach [26]: the abundance of halos at fixed mass is proportional to the probability of the initial density field at a given point first crossing a density threshold  $\delta_{\text{crit}}$  when lowering the smoothing scale from infinity down to the Lagrangian radius  $R(M)$  of those halos. The mean number density of halos  $\bar{n}_h(M)$  is then a function of  $\nu_c = \delta_{\text{crit}}(z)/\sigma(M, z)$ , where  $\sigma(M, z)$  is the square root of the variance of the linear matter density field at redshift  $z$  smoothed on the scale  $R(M)$ . The collapse threshold  $\delta_{\text{crit}}(z) \approx 1.7$  is usually derived as the linearly extrapolated initial spherical overdensity that, when followed fully nonlinearly, collapses at redshift  $z$ . A long-wavelength matter density perturbation  $\delta_\ell$  (in the growing mode) is locally equivalent to reducing the threshold  $\delta_{\text{crit}} \rightarrow \delta_{\text{crit}} - \delta_\ell$ , from which we obtain a prediction for the Lagrangian bias [27, 28]:

$$b_1^L = b_1 - 1 = -\frac{1}{\bar{n}_h(M)} \frac{\partial \bar{n}_h(M)}{\partial \delta_{\text{crit}}}. \quad (14)$$

Thus, if we can derive how the collapse threshold changes under a long-wavelength perturbation in  $\theta_{bc}$  and  $\delta_{bc}$ , we obtain an estimate for  $b_\theta^{bc}$  via

$$b_\theta^{bc} = \frac{1}{\bar{n}_h} \frac{\partial \bar{n}_h}{\partial \theta_{bc}} = -b_1^L \frac{\partial \delta_{\text{crit}}}{\partial \theta_{bc}}, \quad (15)$$

and analogously for  $\delta_{bc}$ .

In order to derive  $\delta_{\text{crit}}$  in the presence of baryon-CDM perturbations, we consider the following setup. We follow a spherical perturbation in the CDM component  $\delta_c$ , which eventually collapses to form a halo at late times. Assuming that Silk damping has erased density perturbations in the baryon component, we take it to be uniform,  $\delta_b = 0$ , until decoupling at  $z(\tau_{\text{dec}}) \simeq 1000$ ; this is a good approximation for the small-scale perturbations that collapse to halos. Note that this does not erase the effect of *large-scale* perturbations in the baryon-CDM ratio  $\delta_{bc}$ , which are still present in the large-scale environment. After decoupling, the baryon fluid is pressureless, but has a *uniform velocity divergence* relative to dark matter; here we set  $\mathbf{v}_{bc} = 0$ , since at leading order the effects of  $\mathbf{v}_{bc}^2$  and  $\theta_{bc}$  decouple.

We further restrict to a tophat (uniform density) perturbation  $\delta_s(\tau)$  of radius  $R_s(\tau)$ ,  $s = c, b$ . Each shell is assumed to be surrounded by space devoid of the corresponding matter component (see Fig. 1) out to a compensation radius  $R_o$ , where

$$R_{o,s}(\tau) = [1 + \delta_s(\tau)]^{1/3} R_s(\tau). \quad (16)$$

Then, the evolution equations reduce to a generalization of the familiar spherical collapse equation,

$$\frac{\ddot{R}_s}{R_s} = -\frac{4\pi G}{3} [\bar{\rho} - 2\rho_\Lambda] - G_s, \quad (17)$$

$$G_s = \sum_{t=c,b} f_t \begin{cases} \delta_t, & R_t \leq R_s \\ \max\{0, (1 + \delta_t)(R_s/R_t)^3 - 1\}, & R_t > R_s \end{cases}$$

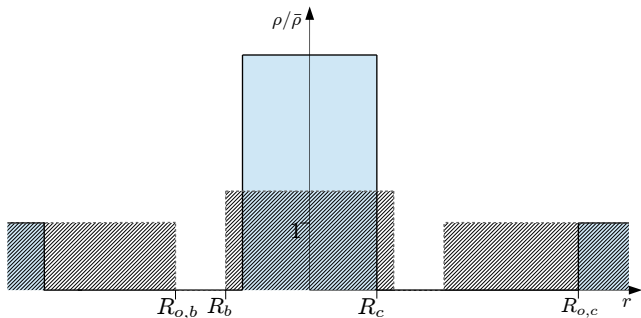


FIG. 1: Illustration of the two-fluid (CDM, solid; baryons, dashed/hatched) spherical collapse setup considered here. The tophat shell radii  $R_b, R_c$  and compensation radii  $R_{o,b}, R_{o,c}$  are indicated. The shells have the same initial radii at  $\tau_{\text{dec}}$ , but different overdensities. In the presence of a relative velocity divergence,  $R_b$  and  $R_c$  evolve differently.

where dots denote derivatives w.r.t. time  $t$  and  $f_t = \Omega_t/\Omega_m$ . Further, during the tophat evolution mass is conserved so that

$$1 + \delta_s(\tau) = [1 + \delta_s(\tau_{\text{in}})] \left( \frac{[R_s/a](\tau)}{[R_s/a](\tau_{\text{in}})} \right)^{-3}. \quad (18)$$

Note that the evolution of two tophat shells with different radii is not consistent; that is, the density profiles will not remain tophat due to the mutual gravitational interaction. We will ignore this effect and simply follow the two shells here. Our results are thus approximate, but sufficient for order-of-magnitude forecasts.

We integrate the equations for  $R_b, R_c$  starting from  $\tau_{\text{in}} = \tau_{\text{dec}}$ . This calculation and the initial conditions, which involve some subtleties, are described in App. B. The initial conditions need some care, since an initial relative velocity divergence  $\theta_{bc}$  can induce an  $R_+$  mode if the latter is not properly nulled. Further, while the overall scale of the tophat perturbation is arbitrary, the ratio  $R_b(\tau_{\text{in}})/R_c(\tau_{\text{in}})$  is not. After decoupling, all baryons within the CDM compensation radius  $R_{o,c}$  [Eq. (16)] depart from their initial velocities and begin to collapse onto the CDM perturbation. Thus, it would seem sensible to choose  $R_b(\tau_{\text{in}}) = R_{o,c}(\tau_{\text{in}})$ . However, one can easily verify that we do not recover linear evolution from the initial conditions unless  $R_b(\tau_{\text{in}}) = R_c(\tau_{\text{in}})$ , an artefact of fixing the tophat shape of the shells. Since the collapse threshold is only meaningful if the tophat density initially follows linear evolution, we thus need to choose  $R_b(\tau_{\text{in}}) = R_c(\tau_{\text{in}})$  (as chosen in [29]). We then adjust  $\delta_{c,\text{in}}$  so that the CDM shell reaches  $R_c = 0$  at the desired redshift  $z_{\text{coll}}$ ; following the baryon shell leads to identical results, since the two are comoving in the late stages of collapse. The collapse threshold  $\delta_{\text{crit}}$  is obtained by integrating the linear growth equation for  $\delta_m$  with the same initial conditions to the same redshift  $z_{\text{coll}}$ . Note that one has to use the linear total matter perturbation since this is what  $\sigma(M, z)$  refers to in the definition of  $\nu_c$ .

We begin with the case  $\delta_{bc} \neq 0$  while  $\theta_{bc} = 0$ ; this

can be implemented by changing  $f_b$  in Eq. (17). By construction,  $R_b = R_c$  initially while in this case we also have  $\dot{R}_b = \dot{R}_c$ . From Eq. (17) we see that the force acting on both shells is the same and hence  $R_b(\tau) = R_c(\tau)$  holds at all times. This means that the  $R_+$ -mode  $\delta_{bc}$  remains constant not only at linear order, but throughout the nonlinear tophat evolution. Hence, a constant compensated density perturbation does not change the collapse threshold,  $\partial\delta_{\text{crit}}/\partial\delta_{bc} = 0$ . This is again an artefact of the double tophat; one can show that  $\delta_r$  no longer remains constant at second order in perturbation theory [i.e., by solving Eq. (33) below]. In any case, the local baryon-CDM ratio is still modified, and we expect an order unity  $b_\theta^{bc}$  for galaxies following Sec. II A.

We now turn to the response of  $\delta_{\text{crit}}$  to  $\theta_{bc}$ . In this case, even though we start with  $R_b = R_c$  at  $\tau_{\text{dec}}$ , we have  $\dot{R}_b - \dot{R}_c \propto \theta_{bc}$  so that the shells evolve differently. This in turn leads to a nontrivial gravitational coupling between the two shells which influences the collapse. Fig. 6 in App. B (filled triangles) shows  $\delta_{\text{crit}}$  as a function of  $\theta_{bc}$ . We fit a linear relation in the range  $|\theta_{bc,0}/H_0| \leq 2 \cdot 10^{-7}$ , and obtain

$$\frac{\partial\delta_{\text{crit}}}{\partial(\theta_{bc,0}/H_0)} = -6.8 \quad \text{at } z = 1.2, \quad (19)$$

with a very small redshift evolution from  $-7.1$  at  $z = 0$  to  $-6.4$  at  $z = 10$ .<sup>3</sup> The slope is negative, meaning that the collapse threshold is lower when baryons fall onto the overdensity with a smaller initial infall velocity than the CDM which is in the growing mode. This might seem counterintuitive. Note however that the growth suppression due to  $\theta_{bc}$  is also contained in the linear growth used to extrapolate  $\delta_{\text{crit}}$  to low redshifts. Thus, the negative slope says that the fractional suppression in the nonlinear growth is smaller than that in the linear growth (similar results have been found for modified gravity in e.g. [30], where growth is enhanced but  $\delta_{\text{crit}}$  is reduced).

Eq. (15) then immediately yields our estimate for  $b_\theta^{bc}$ ,

$$b_\theta^{bc}(z) = [(1+z)H_0]^{-1} \frac{\partial\delta_{\text{crit}}(z)}{\partial(\theta_{bc,0}/H_0)} (1 - b_1) \approx 6.8[(1+z)H_0]^{-1} (b_1 - 1). \quad (20)$$

Clearly, this is of the same order of magnitude as estimated using the simple local bias ansatz in Sec. II A. However, we now have a more precise number, which yields an enhancement of a factor  $\sim 7(b_1 - 1)$ , as well as a prediction for the scaling with  $b_1$  and with redshift. Eq. (20) is the fiducial value we will assume for our results in Sec. II D and Sec. III B.

<sup>3</sup> This result is smaller by a factor  $\sim 10$  than the number given in a previous arXiv version of this paper. The differences resulting in this change are described in App. B.

### C. Induced bias from streaming velocity

The estimates for  $b_\theta^{bc}$  provided so far model the bulk flow effect of a relative velocity divergence. Ref. [14] argued for a  $b_\theta^{bc}$  induced by the relative velocity effect  $\propto \mathbf{v}_{bc}^2$  on very low-mass halos. Specifically, they derived

$$b_\theta^B = \frac{2}{3} b_{v^2} L_s(z) \sigma_{vbc}^{-1}(z) \approx 52 H_0^{-1} \left( \frac{b_{v^2}}{0.01} \right) \left( \frac{D(z)}{D(1.2)} \frac{2.2}{1+z} \right) \quad (21)$$

where

$$L_s(z) \equiv \sigma_{vbc}^{-1}(z) \left\langle v_{bc}^i \frac{\partial_i}{\nabla^2} \delta \right\rangle = \sigma_{vbc}^{-1}(z) \int_{\mathbf{k}} k^{-2} P_{\delta\theta_{bc}}(k, z) \approx 5.34 h^{-1} \text{Mpc} \left( \frac{D(z)}{D(1.2)} \right). \quad (22)$$

Here, we have introduced  $\int_{\mathbf{k}} \equiv \int d^3\mathbf{k}/(2\pi)^3$  and normalized to  $z = 1.2$ . This result was taken from a perturbation theory loop integral (see Sec. IIIB). At  $z = 1.2$  and for a fiducial value of  $b_{v^2} = 0.01$ , this is roughly 8 times larger than the bias predicted from the excursion set Eq. (20) for  $b_1 = 2$ . Note also the very different redshift scalings, where the prediction of Eq. (20) scales as  $b_\theta \propto b_1(z)(1+z)^{-1}$ , while Eq. (21) scales as  $D(z)/(1+z)$ .

Crucially, as discussed in Sec. IIIB below, the loop integral leading to  $b_\theta^B$  runs over very small-scale modes that are not modeled correctly in perturbation theory. In a consistent perturbative expansion, it is absorbed by a renormalized bias parameter  $b_\theta$ , whose value is not calculable within perturbation theory and must be estimated using models of galaxy and halo formation (such as the excursion set). Still, it is reasonable to wonder whether there is in fact a physical contribution to  $b_\theta$  that comes from the relative velocity effect  $\propto v_{bc}^2$ , and is thus related to  $b_{v^2}$ . Such a contribution would be physically independent from, and presumably additive to, the bulk velocity divergence effect estimated using the spherical collapse calculation above. We now derive which properties this contribution would have to have.

Consider a galaxy sample whose local number density  $n_g$  depends, at a given time  $\tau$  and among various other quantities, on  $v_{bc}^2$ . Specifically, we allow for  $n_g(\mathbf{x})$  to depend on  $v_{bc}^2$  in a finite region around  $\mathbf{x}$ :

$$n_g(\mathbf{x}) = \int d^3\mathbf{y} \cdots F_g[v_{bc}^2(\mathbf{x} + \mathbf{y}), \cdots; \mathbf{y}]. \quad (23)$$

Here, the ellipsis stands for other terms such as  $\delta_m(\mathbf{y}')$ , which each come with an associated convolution integral  $\int d^3\mathbf{y}'$ . We are interested in the linear response of  $n_g$  to a long-wavelength perturbation in the relative velocity,  $\mathbf{v}_{bc}^\ell$ . Hence, we write

$$\mathbf{v}_{bc} = \mathbf{v}_{bc}^\ell + \mathbf{v}_{bc}^s, \quad (24)$$

separating the long- and short-wavelength pieces. At leading order,  $\mathbf{v}_{bc}^s$  is uncorrelated with  $\mathbf{v}_{bc}^\ell$ . Further, we

are interested in long-wavelength perturbations that are much larger than the scale  $R_*$  over which galaxies form. In the present context,  $R_*$  is the typical extent of the support of the functional kernel  $F_g$  in Eq. (23). Then, we can perform a Taylor series up to second order in  $\mathbf{v}_{bc}$  to obtain

$$\begin{aligned} n_g(\mathbf{x}) \Big|_{\mathbf{v}_{bc}^\ell} - n_g(\mathbf{x}) \Big|_0 &= \int d^3\mathbf{y} \left( \frac{\partial}{\partial \mathbf{v}_{bc}^2} F_g[0, \cdots; \mathbf{y}] \right) 2\mathbf{v}_{bc}^s(\mathbf{x} + \mathbf{y}) \cdot \mathbf{v}_{bc}^\ell(\mathbf{x} + \mathbf{y}) \\ &\quad + \int d^3\mathbf{y} \left( \frac{\partial}{\partial \mathbf{v}_{bc}^2} F_g[0, \cdots; \mathbf{y}] \right) [\mathbf{v}_{bc}^\ell(\mathbf{x} + \mathbf{y})]^2 \\ &= \int d^3\mathbf{y} \left( \frac{\partial}{\partial \mathbf{v}_{bc}^2} F_g[0, \cdots; \mathbf{y}] \right) \mathbf{v}_{bc}^s(\mathbf{x} + \mathbf{y}) \cdot \mathbf{y} \times \theta_{bc}^\ell(\mathbf{x}) \\ &\quad + \int d^3\mathbf{y} \left( \frac{\partial}{\partial \mathbf{v}_{bc}^2} F_g[0, \cdots; \mathbf{y}] \right) \times (\mathbf{v}_{bc}^\ell)^2(\mathbf{x}) \\ &\quad + \mathcal{O}([\mathbf{v}_{bc}^\ell]^3, \nabla^2 \theta_{bc}^\ell). \end{aligned} \quad (25)$$

In the second line, we have used

$$(\mathbf{v}_{bc}^\ell)^i(\mathbf{x} + \mathbf{y}) = (\mathbf{v}_{bc}^\ell)^i(\mathbf{x}) + y^k \partial_k (\mathbf{v}_{bc}^\ell)^i(\mathbf{x}) + \cdots. \quad (26)$$

The first term vanishes at linear order when inserted into the functional, while of the second term  $\propto \partial_k (\mathbf{v}_{bc}^\ell)^i$  only the trace part, namely  $\theta_{bc}^\ell$  remains, in both cases due to the absence of preferred directions in the small-scale modes. We have dropped higher derivative terms, which we will justify below. We clearly obtain a bias with respect to  $\mathbf{v}_{bc}^2$ , given by the ensemble average of the second line of Eq. (25) over small-scale modes while keeping large-scale modes fixed:

$$b_{v^2}^{bc} = \frac{1}{\bar{n}_g} \left\langle \int d^3\mathbf{y} \cdots \left( \frac{\partial}{\partial \mathbf{v}_{bc}^2} F_g[0, \cdots; \mathbf{y}] \right) \right\rangle. \quad (27)$$

In addition, the first line of Eq. (25) corresponds to an effective bias w.r.t  $\theta_{bc}$ , which we denote as  $b_\theta^{bc, v^2}$ , which is analogously given by

$$b_\theta^{bc, v^2} = \frac{1}{\bar{n}_g} \left\langle \int d^3\mathbf{y} \cdots \left( \frac{\partial}{\partial \mathbf{v}_{bc}^2} F_g[0, \cdots; \mathbf{y}] \right) \mathbf{v}_{bc}(\mathbf{y}) \cdot \mathbf{y} \right\rangle.$$

Here, we can set  $\mathbf{x} \rightarrow 0$ , since the expectation value is independent of position. We also no longer need to explicitly restrict to the small-scale component of  $\mathbf{v}_{bc}$ . Note that to obtain a nonzero value, we need to include the dependence of  $F_g$  on at least one other perturbation (as the expectation value of any fixed integral over  $\mathbf{v}_{bc}$  vanishes). The leading expression is obtained by including a dependence on the local matter density perturbation  $\delta_m$ ,  $F_g \rightarrow F_g[v_{bc}^2, \delta_m; \mathbf{y}, \mathbf{y}']$ . Eq. (23) now becomes a functional in both  $\mathbf{v}_{bc}^2$  and  $\delta_m$ , and the leading term is

$$\begin{aligned} b_\theta^{bc, v^2} &= \frac{1}{\bar{n}_g} \int d^3\mathbf{y} \int d^3\mathbf{y}' \left( \frac{\partial^2}{\partial \mathbf{v}_{bc}^2 \partial \delta_m} F_g[0, 0; \mathbf{y}, \mathbf{y}'] \right) \\ &\quad \times \langle \delta_m(\mathbf{y}') \mathbf{v}_{bc}(\mathbf{y}) \cdot \mathbf{y} \rangle \\ &\sim b_{v^2}^{bc} \langle \delta_m \mathbf{v}_{bc} \cdot \mathbf{y} \rangle_{F_g}. \end{aligned} \quad (28)$$

In the second line of Eq. (28), we have used that the prefactor is expected to be of the same order of magnitude as  $b_{v_2}^{bc}$  given in Eq. (27), while the expectation value is essentially a generalized second moment (with window function normalized to unity) of  $\delta_m$  and  $\mathbf{v}_{bc} \cdot \mathbf{y}$  on the scale  $R_*$ . The physical interpretation of this expression is the following. The number density of observed galaxies depends on the distribution of  $v_{bc}^2(\mathbf{y})$  within a volume of scale  $R_*$ , for example via the effect  $\mathbf{v}_{bc}^2$  has on the abundance of very low-mass halos. The bias  $b_{v_2}^{bc}$  corresponds to the volume average of this dependence (the fact that  $b_{v_2}^{bc}$  quantifies an average over very small-scale effects at high redshifts is the reason for the significant uncertainty in its magnitude). Now, a long-wavelength relative velocity divergence  $\theta_{bc}$  induces a nontrivial radial profile in  $v_{bc}^2$ . This profile depends on the small-scale contributions to  $v_{bc}$ , and thus averages to zero in the absence of other perturbations. However, the small-scale relative velocity correlates with small-scale density perturbations, i.e. regions within the volume  $\sim R_*^3$  considered with large density contrast also have larger amplitudes of the relative velocity on average, and this leads to a net effect of the induced relative velocity profile and hence  $\theta_{bc}$  on the galaxy abundance.

In order to obtain a quantitative estimate, we work to lowest order in perturbation theory, where  $\delta_m, \mathbf{v}_{bc}$  are Gaussian fields. Then, the moment in the last line of Eq. (28) can always be written as

$$\langle \delta_m \mathbf{v}_{bc} \cdot \mathbf{y} \rangle_{F_g} = R_* \int_0^\infty \frac{k^2 dk}{2\pi^2} W_{F_g}(k) k^{-1} P_{\delta\theta_{bc}}(k), \quad (29)$$

where  $W_{F_g}(k)$  is dimensionless and we have pulled out a factor  $R_*$  since by assumption  $|\mathbf{y}|$  is of order  $R_*$ . If  $F_g$  is a smooth function as expected physically, then  $W_{F_g}(k)$  will drop off quickly for  $k \gg 1/R_*$ . Furthermore, low- $k$  modes with  $k \ll 1/R_*$  also cannot contribute to Eq. (29), since the angle average over  $\mathbf{v}_{bc} \cdot \mathbf{y}$  for a constant  $\mathbf{v}_{bc}$  vanishes. Thus, in the limit  $kR_* \ll 1$ , the kernel has to scale as  $W_{F_g}(k) = \mathcal{O}(k^2 R_*^2)$ ; this is easily verified with concrete example kernels in Eq. (28). This means that only modes with  $k$  of order  $R_*$  will contribute appreciably to Eq. (29). Note that this is completely generic, and follows directly from the derivative expansion in Eq. (25). That is, any small-scale modes of  $\mathbf{v}_{bc}$  that contribute to the physical bias parameter  $b_\theta^{bc}$  cannot be of much larger scale than  $R_*$ . This continues to hold if one continues the expansion in derivatives in Eq. (25) to higher order (yielding terms of order  $R_*^{2n} \partial^{2n} \theta_{bc}$ ), and is another qualitative difference to Eqs. (21)–(22).

In summary, we obtain as an order-of-magnitude estimate

$$\begin{aligned} b_\theta^{bc, v^2} &\sim b_{v_2}^{bc} \left( \frac{k^2 P_{\delta\theta_{bc}}(k)}{2\pi^2} \right)_{k \sim \pi/R_*} R_* \\ &\sim 6H_0^{-1} \left( \frac{b_{v_2}^2}{0.01 \sigma_{v_{bc}}^2} \right) \text{ for } R_* \approx 5 h^{-1} \text{ Mpc}, z = 1.2. \end{aligned} \quad (30)$$

Fig. 2 (shaded band) shows the estimate for  $b_\theta^{bc, v^2}$  as

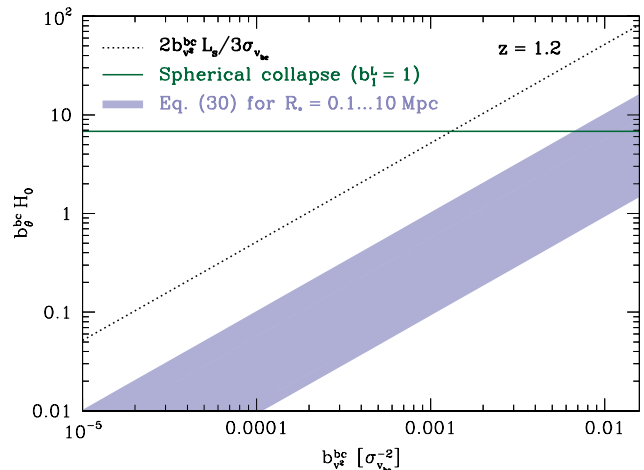


FIG. 2: Various estimates of the bias parameter  $b_\theta^{bc}$  as a function of  $b_{v_2}^{bc}$ . The solid line shows the excursion set estimate Eq. (20) from Sec. II B, which is independent of  $b_{v_2}^{bc}$ . The shaded band shows the rough range of values expected for the induced bias from streaming velocity effects on small scales [Eq. (30)]. The dotted line shows the loop integral derived in [14] [Eq. (21)] which is argued to be unphysical.

a function of  $b_{v_2}^{bc}$  for a range of spatial scales  $R_* = 0.1 - 10 h^{-1}$  Mpc. Since  $k^2 P_{\delta\theta_{bc}}(k)$  shows significant oscillations, we average it over  $k$  with a Gaussian kernel centered on  $\pi/R_*$  and with 1D RMS of  $2\pi/R_*$ , rather than taking the value at exactly  $\pi/R_*$ . In any case, our estimate of  $b_\theta^{bc, v^2}$  can only be taken as a rough approximation. Fig. 2 also shows the estimate Eq. (20) from the previous section, and the result from the loop integral Eq. (21). Clearly, the latter is much larger than either of the two physical estimates if  $b_{v_2}^{bc} \gtrsim 10^{-3}$ . The reason is that the integral in Eq. (22) extends over all modes (in particular large-scale modes with  $k \ll 1/R_*$ ), while we have argued that physically, only modes with  $k$  around  $1/R_*$  should contribute. Whether the contribution  $b_\theta^{bc, v^2}$  dominates over the bulk flow contribution Eq. (20) clearly depends on the value of  $b_{v_2}^{bc}$ ; however, for most of the open parameter space of  $b_{v_2}^{bc}$  the contribution from Eq. (20) is larger.

#### D. Galaxy power spectrum at linear order

Using Eq. (9), we can immediately write down the contributions from baryon-CDM perturbations to the linear galaxy auto and galaxy-matter cross power spectrum:

$$\begin{aligned} P_{gg}^{\text{lin}}(k) \Big|_{bc} &= 2b_1 b_\theta^{bc} P_{\delta\theta_{bc}}(k) + 2b_1 b_\delta^{bc} P_{\delta\delta_{bc}}(k) + (b_\theta^{bc})^2 P_{\theta_{bc}\theta_{bc}}(k) \\ &\quad + (b_\delta^{bc})^2 P_{\delta_{bc}\delta_{bc}}(k) + 2b_\delta^{bc} b_\theta^{bc} P_{\delta_{bc}\theta_{bc}}(k) \\ P_{gm}^{\text{lin}}(k) \Big|_{bc} &= b_\theta^{bc} P_{\delta\theta_{bc}}(k) + b_\delta^{bc} P_{\delta\delta_{bc}}(k), \end{aligned} \quad (31)$$

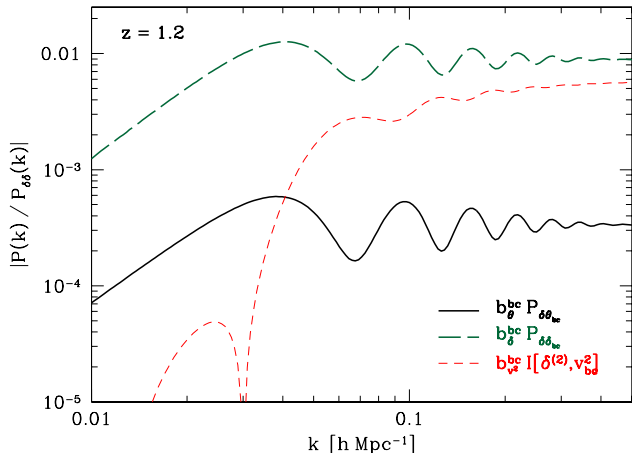


FIG. 3: Leading baryon-CDM perturbation contributions to the galaxy power spectrum (absolute magnitude divided by  $b_1$  at  $z = 1.2$ ), relative to the linear matter power spectrum (solid:  $\theta_{bc}$ ; long-dashed:  $\delta_{bc}$ ). Here we have used  $b_\delta^{bc} = 1$  and  $b_\theta^{bc} = 6.8/[(1+z)H_0]$  [Eq. (20), setting  $b_1 = 2$ ]. We also show the largest of the contributions from the term in Eq. (6),  $b_{v_2}^{bc} \mathcal{I}^{[\delta^{(2)}, v_{bc}^2]}(k)$ , which enter at 1-loop order (short-dashed; Sec. III B), assuming  $b_{v_2}^{bc} = 0.01\sigma_{v_{bc}}^{-2}$ .

where  $P_{xy}(k)$  denote linear cross-power spectra between the matter density ( $\delta$ ), the relative density perturbation ( $\delta_{bc} = R_+$ ) and the relative velocity divergence ( $\theta_{bc} = R_- H_0$ ). Fig. 3 shows the leading contributions, i.e. those involving only one power of  $\delta_{bc}$ ,  $\theta_{bc}$ , divided by  $b_1$  and the linear matter power spectrum  $P_{\delta\delta}(k)$ , at  $z = 1.2$ . We use the transfer function output of CAMB [24], from which we obtain  $R_+$ ,  $R_-$  via the matching described in App. A. Note that both  $\delta_{bc}$  and  $\theta_{bc}$  contributions have a very similar scale dependence. Clearly, despite the large value of  $b_\theta^{bc}$  as compared to  $b_\delta^{bc}$ , the baryon-CDM density perturbation  $\delta_{bc}$  is by far the largest contribution, being roughly scale independent for  $k \gtrsim 0.05 h \text{ Mpc}^{-1}$  at the level of  $\sim 1\%$ . Given that the correlation coefficient of all the fields  $\delta$ ,  $\delta_{bc}$ ,  $\theta_{bc}$  is unity, we also infer immediately that the contributions in Eq. (31) involving two powers of  $\delta_{bc}$ ,  $\theta_{bc}$  are highly suppressed, and contribute at most at the  $\sim 0.01\%$  level.

The operator  $v_{bc}^2$  considered in the previous literature, being quadratic, only contributes to  $P_{gg}(k)$ ,  $P_{gm}(k)$  at the 1-loop level. We will turn to this in Sec. III B. Fig. 3 also shows the largest of the 1-loop contributions  $\propto v_{bc}^2$ , assuming a value  $b_{v_2}^{bc} = 0.01\sigma_{v_{bc}}^{-2}$  at the upper end of the expected range. It is clearly larger than the contribution from  $\theta_{bc}$ , but smaller than that from  $\delta_{bc}$ . While these conclusions depend on the values of the various bias parameters, we generically expect  $\delta_{bc}$  to provide the largest baryon-CDM contribution to the galaxy power spectrum. We will discuss the significance of these contributions for the BAO standard ruler in Sec. IV.

### III. GALAXY CLUSTERING AND BARYON-CDM PERTURBATIONS BEYOND LINEAR ORDER

We now generalize the results of the previous section to nonlinear order in perturbation theory. We begin by deriving all operators that have to be included in the bias expansion Eq. (8) of a general galaxy sample in the presence of baryon-CDM perturbations, that is for nonzero  $\delta_{bc}$ ,  $\theta_{bc}$ ,  $v_{bc}$ . We then provide the complete description of the 1-loop galaxy power spectrum, i.e. the leading nonlinear correction to the results of Sec. II D.

#### A. General bias expansion

The complete bias expansion in the case of Gaussian initial conditions and perturbations that are exclusively in the adiabatic growing mode has recently been derived [17, 19]. We will build on those results. To start, let us derive the equations for the nonlinear system of the coupled baryon-CDM fluids, i.e. the nonlinear generalization of Eq. (1). Denoting the velocity of the total matter fluid as  $v_m^i$  and defining the convective time derivative

$$\frac{D}{D\tau} \equiv \frac{\partial}{\partial\tau} + v_m^i \frac{\partial}{\partial x^i}, \quad (32)$$

we obtain (see also [20])

$$\begin{aligned} \frac{D}{D\tau} \delta_s + \theta_s &= -\delta_s \theta_s - g_s v_{bc}^i \partial_i \delta_s \\ \left( \frac{D}{D\tau} + \mathcal{H} \right) \theta_s + \frac{3}{2} \Omega_m \mathcal{H}^2 \delta_m &= -(\partial^i v_s^k)^2 - g_s v_{bc}^i \partial_i \theta_s, \end{aligned} \quad (33)$$

where  $s = b, c$  and we have introduced the shorthand  $g_b = 1 - f_b$  and  $g_c = -f_b$ . On the l.h.s. we now have the standard differential operator for the gravitational evolution, while the r.h.s. contains the nonlinear terms due to gravitational evolution and the relative velocity. It is clear that  $\delta_m$ ,  $\theta_m$  and the relative density and velocity no longer decouple at nonlinear order. Noting that  $D/D\tau$  is invariant under homogeneous but time-dependent translations (boosts), these equations are explicitly boost-invariant. That is, all quantities that appear in Eq. (33) are local observables (note in particular the absence of  $v_m$ ).

Eq. (33) gives us a strong hint as to which operators we should allow to appear in the bias expansion in the two-fluid system. We have to include  $v_{bc}$ ,  $\delta_b$ ,  $\delta_c$  as well as  $\theta_b$ ,  $\theta_c$  and  $\partial^i v_b^j$ ,  $\partial^i v_c^j$  in the bias expansion. Again, it is convenient to decompose these in terms of the adiabatic growing mode  $\delta_m$ ,  $\partial^i v_m^j$  and the baryon-CDM perturbations  $R_+$ ,  $R_-$ . The latter modes are captured in the bias expansion by including

$$R_+(\mathbf{q}) \quad \text{and} \quad R_-^i \equiv \frac{\partial_q^i}{\nabla_q^2} R_-(\mathbf{q}), \quad (34)$$

and higher spatial derivatives of these quantities (but no time derivatives, see below). Here  $\mathbf{q}$  is the Lagrangian coordinate. Evaluating  $R_{\pm}$  at the Lagrangian position is in fact required in order to be able to renormalize the operators consistently [25]. Before proceeding to the general bias expansion, we should consider the importance of spatial derivatives. From Eq. (33) it is clear that  $R_+$  and  $\partial^i R_-^j$  have the same status as  $\delta_m$ ,  $\partial^i v_m^j$ . These terms are thus to be considered as lowest order in derivatives. Higher spatial derivatives, for example  $\partial^k R_+$  or  $\nabla^2 R_-^i$  are then expected to be suppressed by the same scale that appears in higher derivative operators of the adiabatic quantities, for example  $\partial^k \delta_m$ . This is the spatial scale  $R_*$ , which for halos is of order the Lagrangian radius, or smaller.

Let us now derive the complete set of operators of the bias expansion at lowest order in derivatives. Formally, this is what is obtained in the limit  $R_* \rightarrow 0$ . We begin with a recap of the adiabatic growing mode case. The basis of operators in this case can be conveniently constructed out of the tidal tensor  $\Pi_{ij}^{[1]} \equiv 2\partial_i \partial_j \Phi / (3\Omega_m \mathcal{H})^2$ , which contains the density (trace part) and tidal field. Here, a superscript  $[n]$  denotes operators that *start* at  $n$ -th order in perturbation theory, while  $n$ -th order *contributions* to an operator are denoted with a superscript  $(n)$ . In addition, we have to include convective time derivatives of  $\Pi_{ij}^{[1]}$ . We then define

$$\Pi_{ij}^{[n]} \equiv \frac{1}{(n-1)!} \left[ (\mathcal{H}f)^{-1} \frac{D}{D\tau} \Pi_{ij}^{[n-1]} - (n-1) \Pi_{ij}^{[n-1]} \right], \quad (35)$$

which by construction is an operator that starts at  $n$ -th order in perturbation theory. The basis then consists of all scalar combinations of the  $\Pi_{ij}^{[n]}$  up to the desired perturbative order, with the exception of  $\text{Tr}[\Pi^{[n]}]$ ,  $n > 1$ , which is expressible in terms of lower order operators [17]. For example, up to third order, we then have the following list of bias operators for Gaussian initial conditions [17]:

$$\begin{aligned} 1^{\text{st}} & \quad \text{Tr}[\Pi^{[1]}] \\ 2^{\text{nd}} & \quad \text{Tr}[(\Pi^{[1]})^2], (\text{Tr}[\Pi^{[1]}])^2 \\ 3^{\text{rd}} & \quad \text{Tr}[(\Pi^{[1]})^3], \text{Tr}[(\Pi^{[1]})^2] \text{Tr}[\Pi^{[1]}], (\text{Tr}[\Pi^{[1]}])^3, \\ & \quad \text{Tr}[\Pi^{[1]} \Pi^{[2]}], \end{aligned} \quad (36)$$

where all operators are evaluated at the same Eulerian position and time  $(\mathbf{x}, \tau)$ . These are simply all scalar combinations of the matter density and tidal field, with the exception of the last term in the third line which involves a time derivative and is, at a fixed time, nonlocally related to the density and tidal field [17, 19].

We now simply augment the list Eq. (36) by all scalar combinations of  $\Pi_{ij}^{[n]}$  with  $R_+$ ,  $R_-^i$ ,  $\partial^j R_-^i$ . Unlike for the quantities  $\delta_m$ ,  $\partial^i v_m^j$  which grow under gravity, we do not have to consider time derivatives of  $R_+$  and  $R_-^i$  in the bias expansion, since these perturbations are merely set

in the initial conditions. This is similar to the case of non-Gaussian initial conditions, where an additional field  $\phi(\mathbf{q})$  appears in the bias expansion, again without time derivatives [25]. Note that, once all terms at a given order are included, we can equivalently consider the derivatives acting on  $R_-$  [Eq. (34)] as being with respect to Eulerian coordinate  $\mathbf{x}$ , since the Jacobian  $\partial \mathbf{x}^i / \partial \mathbf{q}^j$  is expressible in terms of the other terms included in the general bias expansion. Defining  $\mathbf{R}_- = R_-^i$ , and adopting matrix notation (where  $R_-$  stands for  $\partial^i R_-^j$ ), we have to augment the list Eq. (36) up to cubic order by

$$\begin{aligned} 1^{\text{st}} & \quad R_+(\mathbf{q}), \text{Tr}[\mathbf{R}_-](\mathbf{q}) \\ 2^{\text{nd}} & \quad R_+ \text{Tr}[\Pi^{[1]}], (\mathbf{R}_-)^2, \text{Tr}[\mathbf{R}_- \Pi^{[1]}], \text{Tr}[\mathbf{R}_-] \text{Tr}[\Pi^{[1]}] \\ 3^{\text{rd}} & \quad R_+ \text{Tr}[(\Pi^{[1]})^2], R_+ (\text{Tr}[\Pi^{[1]})^2], (\mathbf{R}_-)^2 \text{Tr}[\Pi^{[1]}], \\ & \quad \mathbf{R}_- \Pi^{[1]} \mathbf{R}_-, \text{Tr}[\mathbf{R}_- (\Pi^{[1]})^2], \text{Tr}[\mathbf{R}_- \Pi^{[1]}] \text{Tr}[\Pi^{[1]}], \\ & \quad \text{Tr}[\mathbf{R}_-] \text{Tr}[(\Pi^{[1]})^2], \text{Tr}[\mathbf{R}_-] (\text{Tr}[\Pi^{[1]})^2], \text{Tr}[\mathbf{R}_- \Pi^{[2]}], \end{aligned} \quad (37)$$

where  $R_{\pm}$  are all evaluated at the Lagrangian position  $\mathbf{q}[\mathbf{x}, \tau]$  while  $\Pi_{ij}^{[n]}$  are evaluated at  $(\mathbf{x}, \tau)$ . Here, we have restricted to terms that are linear in  $R_{\pm}$ . However, we have kept terms involving  $(R_-^i)^2 \propto v_{bc}^2$ . The reasoning is that there is possibly a hierarchy between  $b_{v^2}^{bc}$  and  $b_{\delta}^{bc}$ ,  $b_{\theta}^{bc}$  as we have seen in Sec. II. Fig. 3 shows that the terms that are higher order in  $R_{\pm}$  will be highly suppressed (although it is straightforward to include them). Further, following our discussion about higher derivatives, we neglect the term  $R_-^i \partial_i \delta$ , since its bias parameter is expected to be of order  $R_*$ , whereas the coefficient multiplying  $\partial_i R_-^i \delta$  is of order  $H_0^{-1}$  [Eq. (20)].

We can equivalently express the list in Eq. (37) in a slightly more familiar form, in terms of the matter density and tidal field  $K_{ij} \equiv (\partial_i \partial_j / \nabla^2 - \delta_{ij} / 3) \delta_m$ ,

$$\begin{aligned} 1^{\text{st}} & \quad \delta_{bc}, \theta_{bc} \\ 2^{\text{nd}} & \quad \delta_{bc} \delta, v_{bc}^2, \theta_{bc} \delta, K_{ij} \partial^i v_{bc}^j \\ 3^{\text{rd}} & \quad \delta_{bc} \delta^2, \delta_{bc} (K_{ij})^2, v_{bc}^2 \delta, K_{ij} v_{bc}^i v_{bc}^j, \theta_{bc} \delta^2, \theta_{bc} (K_{ij})^2, \\ & \quad \delta K_{ij} \partial^i v_{bc}^j, K_{ij} K_{kl}^j \partial^i v_{bc}^k, O_{\text{nloc}}^{bc}, \end{aligned} \quad (38)$$

where from now on we let  $\delta \equiv \delta_m$  for clarity, and

$$O_{\text{nloc}}^{bc} \equiv \frac{8}{21} \left( \partial^i v_{bc}^j - \frac{1}{3} \delta^{ij} \theta_{bc} \right) \frac{\partial_i \partial_j}{\nabla^2} \left[ \delta^2 - \frac{3}{2} (K_{lm})^2 \right].$$

Up to other cubic terms already included in Eq. (38),  $O_{\text{nloc}}^{bc}$  can also be written as  $(4/5) \text{Tr}[\mathbf{R}_- \Pi^{[2]}]$ . It is clearly nonlocally related to  $\delta$ ,  $K_{ij}$ . This is the first instance of a convective time derivative appearing in the bias expansion. Equivalently, it can be seen as a generalization of  $\Gamma_3$  defined in [16].

Apart from  $v_{bc}^2$  [9, 10],  $\delta_{bc}$  [3], and  $\theta_{bc}$ ,  $\delta v_{bc}^2$ ,  $K_{ij} v_{bc}^i v_{bc}^j$  [14], all terms in Eqs. (37)–(38) are introduced here for the first time. In general, each of these terms is associated with a respective bias parameter that is specific to any given galaxy sample. However, many of the terms are linked by similar physics, so we can estimate the order of

magnitude of the bias coefficients that are associated to each operator:

(i) *operators involving  $R_+ = \delta_{bc}$* : the coefficients are expected to be of order one, that is of the same order as the ordinary, growing-mode bias parameters multiplying  $\delta$ ,  $(K_{ij})^2, \dots$ . Whether there is an enhancement for rare massive halos like in the case of the density bias parameters is unclear however.

(ii) *operators involving  $v_{bc}^i v_{bc}^j$* : the coefficients of these terms are expected to be of order  $b_{v^2}$ , which as discussed in Sec. I could be as large as  $0.01\sigma_{v_{bc}}^{-2}$ , or as small as  $10^{-5}\sigma_{v_{bc}}^{-2}$ .

(iii) *operators involving  $\partial^i v_{bc}^j$* : these include  $\theta_{bc}$ , and we expect the associated bias parameters to be of similar order as  $b_{\theta}^{bc} \sim \text{few } H_0^{-1}$ .

As we will see in Sec. IIIB, the hierarchy between the bias parameters determines which terms are the most relevant in the prediction for galaxy statistics. The potential large magnitude of  $b_{v^2}^{bc}$  compared to what is expected for the other two classes of terms was already used in Eqs. (37)–(38), where we keep terms with two powers of  $v_{bc}^i$  but only one power of  $\delta_{bc}$ ,  $\partial^i v_{bc}^j$ .

In addition to the deterministic operators listed in Eqs. (37)–(38), there are also stochastic contributions induced by integrating out the small-scale perturbations; physically, two galaxies in the same large-scale environment form from different realizations of the small-scale density field and their properties will correspondingly scatter around the expectation value. This can be taken into account consistently in the bias expansion by introducing stochastic fields  $\epsilon_O$  for each operator in the list Eqs. (36)–(37) [17], where  $\epsilon_O$  have zero mean and are at lowest order in derivatives fully characterized by their one-point moments. Note that for an  $n$ -th order operator  $O^{[n]}$ , these terms are order  $n+1$  in perturbation theory. Further, in case of the galaxy two-point function, these terms are fully captured by including ‘‘contact terms’’  $P_g(k) \supset N_0 + N_2(R_*k)^2 + N_4(R_*k)^4 + \dots$  [16], which are already present in the absence of baryon-CDM perturbations. Thus, baryon-CDM perturbations do not add new stochastic contributions at the two-point function level.

Further, Eqs. (37)–(38) are only complete at lowest order in spatial derivatives. The fact that galaxy formation is not perfectly local induces additional operators with higher spatial derivatives. Essentially, we have to allow for any scalar combination of  $\partial \dots \partial \Pi_{ij}^{[n]}$ ,  $\partial \dots \partial R_+$ , and  $\partial \dots \partial R_-^i$ . Each derivative comes with the spatial scale  $R_*$  of galaxy formation. The two leading higher-derivative operators are

$$R_*^2 \nabla^2 \delta_{bc}, \quad R_*^2 \nabla^2 \theta_{bc}. \quad (39)$$

Note that we have already included all first order derivatives of  $v_{bc}^i$  in Eqs. (37)–(38), as they are not necessarily suppressed by  $R_*$  (nevertheless, these terms could contain contributions induced by the nonlocality of galaxy formation, as described in Sec. IIC). Higher-derivative terms generally become relevant on small scales. For

example, for values of  $R_* \lesssim 10 h^{-1} \text{ Mpc}$ , the terms in Eq. (39) are comparable to the next-to-leading contributions from higher order bias terms (see Sec. IIIB).

Finally, as noted by [14], the fact that  $R_{\pm}$  are evaluated at the Lagrangian position introduces further terms (again this is analogous to the case for primordial non-Gaussianity [25, 31]),

$$\begin{aligned} 2^{\text{nd}} : & -s^k \partial_k \delta_{bc}, \quad -s^k \partial_k \theta_{bc} \\ 3^{\text{d}} : & \frac{1}{2} s^l s^k \partial_l \partial_k \delta_{bc}, \quad \frac{1}{2} s^l s^k \partial_l \partial_k \theta_{bc}, \quad -s^k \partial_k v_{bc}^2, \\ & -\delta s^k \partial_k \delta_{bc}, \quad -\delta s^k \partial_k \theta_{bc}, \quad -s^k K_{ij} \partial_k \partial^i v_{bc}^j, \end{aligned} \quad (40)$$

where  $s$  is the displacement from the Lagrangian to Eulerian position, given by  $s^i = -\partial^i / \nabla^2 \delta$  at linear order. Each term in Eq. (40) is multiplied by the bias parameter of the corresponding leading operator in Eq. (38). They thus do not introduce additional free parameters.

## B. Galaxy power spectrum at 1-loop order

In order to derive the next-to-leading 1-loop contribution to the galaxy power spectrum, we need to go to third order in perturbation theory, and consequently need to consider all terms given in Eq. (38). Throughout, we only keep terms at linear order in  $\delta_{bc}$ ,  $\theta_{bc}$ , as the higher order terms are highly suppressed (Sec. IID), but keep quadratic terms in  $v_{bc}^2$ ; the extension to include all non-linear terms in  $\delta_{bc}$ ,  $\theta_{bc}$  is straightforward.

Before presenting the calculation, we begin with some general considerations. The 1-loop contributions to  $P_{gg}$ ,  $P_{gm}$  involve an integral  $\int_{\mathbf{p}} \equiv \int d^3 \mathbf{p} / (2\pi)^3$  over a loop momentum which can include contributions from very small scales. Whether the integral converges to a finite value or not, these scales are not modeled physically by perturbation theory. Instead, these contributions need to be isolated and removed, a procedure known from field theory as renormalization [16, 32]. This can be done by introducing an artificial cutoff  $\Lambda$  and then adding counterterms to cancel the cutoff-dependent loop contributions. The end result is that unphysical contributions are absorbed in renormalized bias parameters of lower order terms (or stochastic terms). In the following we will describe this briefly in the context of the baryon-CDM contributions. For this, we divide the terms in Eq. (38) into two classes.

(i) terms constructed out of  $\delta_{bc}$ ,  $\theta_{bc}$  and  $\partial^i v_{bc}^j$  together with  $\delta$  and  $K_{ij}$ : these have the same structure as those present in standard perturbation theory, and we can use results of the latter by simply replacing  $P_{\delta\delta}(k)$  with  $P_{\delta\delta_{bc}}(k)$  or  $P_{\delta\theta_{bc}}(k)$ , as appropriate, in the loop integrals. As shown in [16, 32], the only terms that remain after renormalization of the 1-loop galaxy power spectrum are  $\delta^2$ ,  $\mathcal{G}_2 \equiv (K_{ij})^2 - (2/3)\delta^2$ , and  $O_{\text{nlloc}} \propto (4/5) \text{Tr}[\Pi^{[1]}\Pi^{[2]}]$ , so that the corresponding baryon-CDM terms are

$$b_{\delta\delta}^{bc} [\delta_{bc} \delta], \quad b_{\theta\delta}^{bc} [\theta_{bc} \delta], \quad b_{\mathcal{G}}^{bc} [\mathcal{G}^{bc}], \quad b_{\text{nlloc}}^{bc} [O_{\text{nlloc}}^{bc}],$$

where brackets denote renormalized operators and

$$\mathcal{G}^{bc} \equiv K_{ij} \partial^i v_{bc}^j - (2/3) \theta_{bc} \delta. \quad (41)$$

None of these terms has been included in previous calculations of baryon-CDM contributions to galaxy clustering [10–14].

(*ii*) terms constructed out of  $\mathbf{v}_{bc}$  (without derivatives) and/or  $\mathbf{s}$ : these have a different structure, and need to be dealt with separately. Apart from the term  $v_{bc}^2$  considered in [10–14], we also find new contributions from  $s^k \partial_k \theta_{bc}$  and  $s^k \partial_k \delta_{bc}$ . All other terms either vanish by symmetry or renormalize  $b_1$ ,  $b_{\theta}^{bc}$ , or higher derivative terms. Let us briefly consider the term  $s^k \partial_k v_{bc}^2$ , contributing to  $P_{gg}^{1\text{-loop}}$ ,  $P_{gm}^{1\text{-loop}}$  through

$$\begin{aligned} \langle \delta(\mathbf{k}) (s^k \partial_k v_{bc}^2)(\mathbf{k}') \rangle &= 2 \langle \delta(\mathbf{k}) \theta_{bc}(\mathbf{k}') \rangle \int_{\mathbf{p}} \frac{(\mathbf{k} \cdot \mathbf{p})^2}{k^2 p^4} P_{\delta \theta_{bc}}(\mathbf{p}) \\ &= \frac{4}{3} \langle \delta(\mathbf{k}) \theta_{bc}(\mathbf{k}') \rangle \int_{\mathbf{p}} p^{-2} P_{\delta \theta_{bc}}(\mathbf{p}). \end{aligned} \quad (42)$$

This term is absorbed in the tree-level contribution via the renormalized bias coefficient  $b_{\theta}^{bc}$ , since it is given by  $\langle \delta(\mathbf{k}) \theta_{bc}(\mathbf{k}') \rangle$  multiplied by a cutoff-dependent integral [see Eqs. (21)–(22)]. Within renormalized perturbation theory, there is no prediction for the physical bias  $b_{\theta}^{bc}$ , which can only be estimated through toy models of the small-scale physics of galaxy formation. In Sec. II, we have provided several estimates which are summarized in Fig. 2. These are significantly smaller than the fiducial value adopted by [14].

To summarize, at 1-loop order the effects of baryon-CDM perturbations on the galaxy power spectrum are fully generally described by five additional bias parameters:

$$\{b_{v^2}^{bc}, b_{\delta\delta}^{bc}, b_{\delta\theta}^{bc}, b_{\mathcal{G}}^{bc}, b_{\text{nlloc}}^{bc}\}. \quad (43)$$

If we were to include terms of order  $\delta_{bc}^2$ ,  $\theta_{bc}^2$  and higher, this would add another four bias parameters. Extending the notation introduced by [16], we can succinctly summarize the contributions to  $P_{gg}$  as

$$P_{gg}^{1\text{-loop}}(k) \Big|_{bc} = 2b_1 P_{gm}^{1\text{-loop}}(k) \Big|_{bc} + \sum_{O, O'_{bc}} b_O b_{O'_{bc}} \mathcal{I}^{[O, O'_{bc}]}(k),$$

where  $O \in \{\delta^2, \mathcal{G}_2\}$ , while

$$O'_{bc} \in \{v_{bc}^2, \delta\delta_{bc}, \delta\theta_{bc}, \mathcal{G}^{bc}, s^i \partial_i \delta_{bc}, s^i \partial_i \theta_{bc}\}, \quad (44)$$

with  $b_{s\partial\delta_{bc}} \equiv -b_{\delta}^{bc}$ ,  $b_{s\partial\theta_{bc}} \equiv -b_{\theta}^{bc}$ . Finally,  $P_{gm}$  is given

by

$$\begin{aligned} P_{gm}^{1\text{-loop}}(k) \Big|_{bc} &= b_{\delta\delta}^{bc} \mathcal{I}^{[\delta^{[2]}, \delta\delta_{bc}]}(k) + b_{\delta\theta}^{bc} \mathcal{I}^{[\delta^{[2]}, \delta\theta_{bc}]}(k) \\ &\quad - b_{\delta}^{bc} \mathcal{I}^{[\delta^{[2]}, s\partial\delta_{bc}]}(k) - b_{\theta}^{bc} \mathcal{I}^{[\delta^{[2]}, s\partial\theta_{bc}]}(k) \\ &\quad + b_{\mathcal{G}}^{bc} \mathcal{I}^{[\delta^{[2]}, \mathcal{G}^{bc}]}(k) + b_{v^2}^{bc} \mathcal{I}^{[\delta^{[2]}, v_{bc}^2]}(k) \\ &\quad + \left[ \left( b_{\mathcal{G}}^{bc} + \frac{2}{5} b_{\text{nlloc}}^{bc} \right) f_{\theta_{bc}}(k) \right. \\ &\quad \quad \left. - b_{\theta}^{bc} f_{s\partial\theta_{bc}}(k) - b_{\delta}^{bc} f_{s\partial\delta_{bc}}(k) \right] P_{\delta\delta}(k) \\ &\quad + b_{\delta^2}^{bc} k^2 P_{\delta\delta_{bc}}(k) + b_{\delta\theta}^{bc} k^2 P_{\delta\theta_{bc}}(k). \end{aligned} \quad (45)$$

Here we have defined

$$\begin{aligned} f_Y(k) &= 4 \int_{\mathbf{p}} S_{\mathcal{G}_2}(\mathbf{p}, \mathbf{k} - \mathbf{p}) F_2(\mathbf{k}, -\mathbf{p}) P_{\delta Y}(p) \\ f_{s\partial Y}(k) &= -\frac{3}{7} \int_{\mathbf{p}} S_{s\partial\theta_{bc}}(\mathbf{k} - \mathbf{p}, \mathbf{p}) S_{\mathcal{G}_2}(\mathbf{k}, -\mathbf{p}) P_{\delta Y}(p), \end{aligned}$$

where  $Y = \delta_{bc}$ ,  $\theta_{bc}$  and the kernels are given below. Further,

$$\begin{aligned} \mathcal{I}^{[O, O'_{bc}]}(k) &= 2 \int_{\mathbf{p}} S_O(\mathbf{p}, \mathbf{k} - \mathbf{p}) S_{O'_{bc}}(\mathbf{p}, \mathbf{k} - \mathbf{p}) \\ &\quad \times P_{\delta X}(p) [P_{\delta Y}(|\mathbf{k} - \mathbf{p}|) - P_{\delta Y}(p)], \end{aligned} \quad (46)$$

where  $X = \theta_{bc}$  for  $O'_{bc} = v_{bc}^2$ , and  $X = \delta$  otherwise, while  $Y = \theta_{bc}$  for operators involving  $v_{bc}^i$ ,  $\partial^i v_{bc}^j$  and  $Y = \delta_{bc}$  for operators involving  $\delta_{bc}$ .  $F_2$  denotes the symmetrized perturbation theory kernel [33]. Finally, letting  $\mu = \mathbf{k}_1 \cdot \mathbf{k}_2 / (k_1 k_2)$ ,

$$S_O(\mathbf{k}_1, \mathbf{k}_2) = \begin{cases} 1, & O = \delta^2, \delta\delta_{bc}, \delta\theta_{bc} \\ \mu^2 - 1, & O = \mathcal{G}_2, \mathcal{G}^{bc} \\ F_2(\mathbf{k}_1, \mathbf{k}_2), & O = \delta^{[2]} \\ \mu k_2 / k_1, & O = s^i \partial_i \delta_{bc}, s^i \partial_i \theta_{bc} \\ -\mu / (k_1 k_2), & O = v_{bc}^2 \end{cases}.$$

In the definition of  $\mathcal{I}^{[O, O']}$ , we subtract the constant contribution for  $k \rightarrow 0$  that is present for  $O \neq \delta^{[2]}$ , since it renormalizes the galaxy shot noise. Note this is not done in [12], resulting in relatively large unphysical contributions from  $v_{cb}^2$  at low  $k$ . We have neglected any contribution from baryon-CDM perturbations to the matter power spectrum  $P_{mm}(k)|_{bc}$ . At low redshifts, these are expected to be much smaller than those introduced by galaxy biasing [34].

Fig. 4 shows a subset of the terms in  $P_{gg}^{1\text{-loop}}$ . We only show  $\mathcal{I}^{[\delta^{[2]}, O'_{bc}]}$  since these are slightly larger than the others,  $\mathcal{I}^{[\delta^2, O'_{bc}]}$ ,  $\mathcal{I}^{[\mathcal{G}_2, O'_{bc}]}$ , while the scale dependence is essentially identical. The left panel shows terms involving  $v_{bc}^2$ ,  $\partial^i v_{bc}^j$ , while the right panel shows those containing  $\delta_{bc}$ . In the latter case, we also show the leading higher derivative term [last line in Eq. (45)]. Further, we do not show all terms for  $\delta_{bc}$ , since their scale dependence is very similar to that of the corresponding term

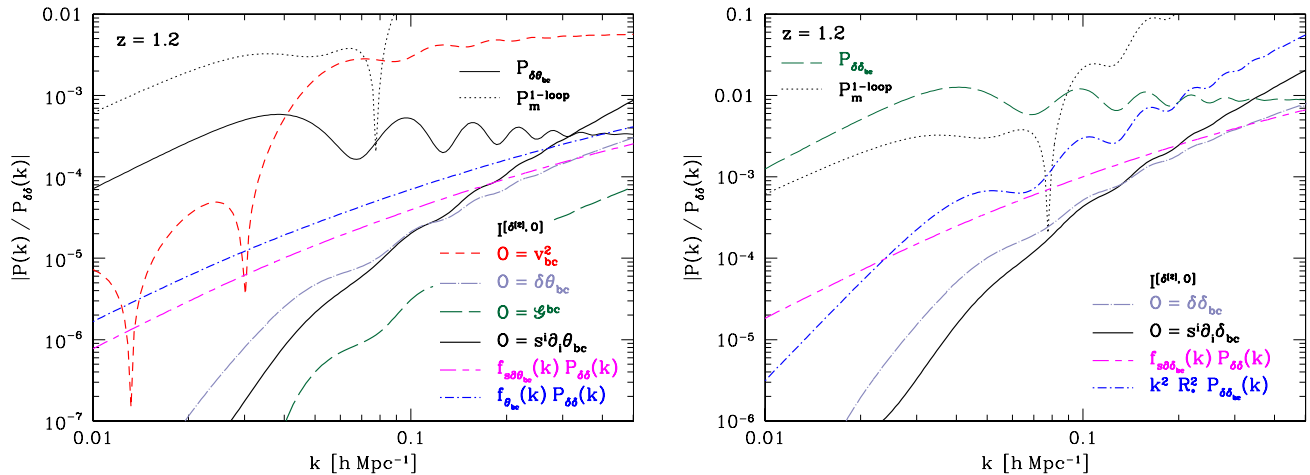


FIG. 4: Baryon-CDM relative velocity ( $\propto \theta_{bc}$ ,  $v_{bc}^2$ , left panel) and density ( $\delta_{bc}$ , right panel; note the different scale) contributions to the galaxy power spectrum at 1-loop order (absolute magnitude at  $z = 1.2$ ), relative to the linear matter power spectrum. Terms involving  $v_{bc}^2$  have been scaled by  $b_{v^2}^{bc} = 0.01\sigma_{v_{bc}}^{-2}(z)$  [Eq. (7)], while terms involving  $\theta_{bc}$ ,  $\partial^i v_{bc}^j$  are scaled with  $b_{\theta}^{bc} = 6.8/[(1+z)H_0]$  [Eq. (20)]. Terms involving  $\delta_{bc}$  in the right panel are scaled with  $b_{\delta}^{bc} = 1$ . For  $\delta_{bc}$ , we also show the leading higher derivative term (magenta short-long-dashed, assuming  $R_* = 5 h^{-1}$  Mpc). For comparison, we also show the corresponding linear order contributions from Fig. 3,  $P_{\delta_{bc}}(k)$  (left) and  $P_{\delta\delta_{bc}}(k)$  (right), respectively, and illustrate the level of standard nonlinear contributions via the matter 1-loop power spectrum (dotted line).

involving  $\theta_{bc}$ . Each term is to be multiplied by one of  $\{b_{\theta}^{bc}, b_{v^2}^{bc}, b_{\delta\theta}^{bc}, b_{\mathcal{G}}^{bc}, b_{\text{nlloc}}^{bc}\}$ , for which we do not have precise individual estimates. Instead, we rely on the scaling described at the end of Sec. III A, multiplying each term by either  $b_{\delta}^{bc} = 1$  (operators  $\propto \delta_{bc}$ ),  $b_{v^2}^{bc}$  (operators  $\propto v_{bc}^2$ ) or  $b_{\theta}^{bc}$  (operators  $\propto \theta_{bc}$ ,  $\partial_i v_{bc}^j$ ). The 1-loop contributions are smaller than the linear order contributions on large scales, while the 1-loop terms involving  $v_{bc}^2$  and  $\theta_{bc}$  are comparable. This validates the counting of baryon-CDM contributions, and confirms that we can neglect the higher order terms in  $\delta_{bc}$ ,  $\theta_{bc}$ . However, note that this ranking assumes  $b_{v^2}^{bc} \sim 0.01\sigma_{v_{bc}}^{-2}$  [Eq. (7)]; a significantly smaller value of  $b_{v^2}^{bc}$  will make the terms  $\propto \theta_{bc}$ ,  $\partial_i v_{bc}^j$  relatively more important.

#### IV. CONCLUSIONS

We have given a complete and consistent perturbative description of the effect of baryon-CDM perturbations on galaxy clustering, showing as most important examples the linear and 1-loop galaxy two-point functions. Three physical effects can be distinguished: the constant compensated mode  $\delta_{bc}$ , which effectively modulates the local baryon fraction; divergence and shear in the relative velocity  $\theta_{bc}$ ,  $\partial^i v_{bc}^j$ , which is a decaying mode; and the relative velocity itself, which enters as  $v_{bc}^2$  at lowest order. Previous literature has mainly focused on this last effect, which enters at subleading order. On the other hand,  $\delta_{bc}$ ,  $\theta_{bc}$  contribute at linear order (Fig. 3). Using physical models of the bias parameters (Sec. II)

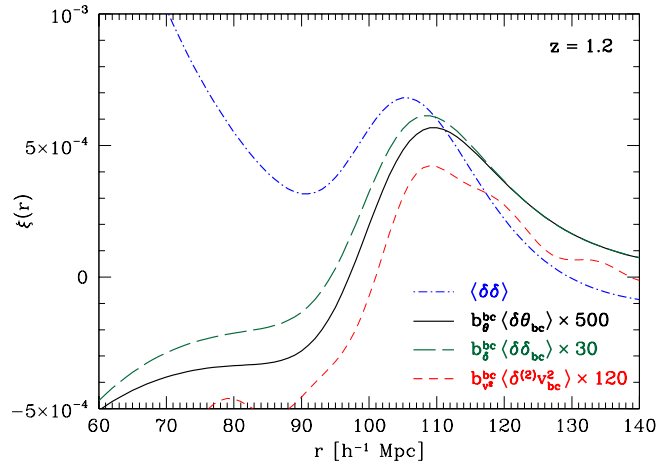


FIG. 5: The three leading contributions  $\propto \delta_{bc}$ ,  $\theta_{bc}$ , and  $v_{bc}^2$  to the galaxy correlation function in real space, i.e. the real-space version of the results shown in Fig. 3 (same line styles). We have scaled each contribution by the number indicated, in order to illustrate the shape and position of the BAO feature in each contribution. The term  $b_{\delta}^{bc} P_{\delta\delta_{bc}}(k)$  is expected to yield the most significant systematic shift of the BAO scale.

for the  $\delta_{bc}$  and  $\theta_{bc}$  contributions, we estimate that the constant compensated mode  $\delta_{bc}$  is the most important baryon-CDM effect on galaxy clustering by a significant margin on large scales. The bias  $b_{v^2}^{bc}$  is the most theoretically uncertain, and this contribution could be either larger or smaller than the velocity divergence effect

$b_\theta^{bc} \sim 7H_0^{-1}(b_1 - 1)/(1 + z)$ . The terms appearing at 1-loop order are generally even smaller than the linear order contributions. However, it is important to include all, if any, of the 1-loop contributions in order to have a consistent model. Sec. IIIB provides all the necessary expressions for this.

Of particular importance are the baryon acoustic oscillation (BAO) features imprinted on the baryon-CDM contributions, which are able to shift the BAO feature in the galaxy power spectrum, and thus systematically bias this standard ruler. Note that this applies to all three contributions  $\propto \delta_{bc}, \theta_{bc}, v_{bc}^2$  shown in Fourier space in Fig. 3. This is illustrated in Fig. 5, which shows these terms in real space. Clearly, all three contributions exhibit a prominent BAO feature that is shifted from that in the growing mode. Nevertheless, none of these contributions is expected to exceed the 1% level, so that current BAO constraints are very likely to be unbiased within error bars. Marginalizing over the leading additional bias parameters introduced here will remove any potential systematic bias introduced by primordial baryon-CDM perturbations in future, larger surveys. For this, physical estimates of the bias parameters such as those presented in Sec. II will be highly useful. Clearly, there is significant room for refining these estimates through both semi-analytical and fully numerical approaches.

### Acknowledgments

I would like to thank Kyungjin Ahn, Jonathan Blazek, Pat McDonald, Mehrdad Mirbabayi, Uroš Seljak, Jaiyul Yoo and Simon White for helpful discussions, and acknowledge support from the Marie Curie Career Integration Grant (FP7-PEOPLE-2013-CIG) ‘‘FundPhysicsAndLSS.’’

### Appendix A: Transfer functions

The linear predictions for the total matter density perturbation as well as the baryon-CDM perturbations can be taken from the Boltzmann solver CAMB [24]. However, some subtleties need to be observed when taking CAMB transfer functions as initial conditions for perturbation theory calculations or N-body simulations. The latter calculations assume matter (or dark energy) domination, and ignore radiation as well as neutrinos, in particular the significant neutrino anisotropic stress at early times. Suppose one took the CAMB transfer function at some high redshift  $z_{\text{in}} \gtrsim 50$ . Then, standard perturbation theory and N-body codes would not yield the correct *linear* evolution of perturbations. Moreover, results will depend on the initial redshift chosen (see [7] for a nice description of this issue). Thus, in order to ensure that the correct linear evolution at low redshifts is recovered, the following procedure should be adopted:

1. Obtain CAMB transfer functions  $T_b(k), T_c(k)$  for baryons and CDM, as well as  $T_{v_{bc}}(k)$  for  $v_{bc}$ , at low redshifts. Here we assume  $z = 0$ .
2. Match to the linear modes derived in Sec. I,

$$R_-(k) = \frac{k}{H_0} \frac{T_{v_{bc}}(k)}{T_m(k)} \delta_m(k, 0)$$

$$R_+(k) = \frac{T_b(k) - T_c(k)}{T_m(k)} \delta_m(k, 0) - R_-(k) D_r(\tau_0),$$

where  $\delta_m(k, z = 0) \propto T_m(k) A_s^{1/2}$ ,  $T_m = f_b T_b + (1 - f_b) T_c$ , is the standard growing-mode total matter density perturbation. In practice, the second term  $\propto R_-$  in  $R_+$  is a small (less than 1%) correction.

3. Using the linear solution that is exact for matter+ $\Lambda$  [Eq. (3)], calculate  $\delta_m(k, z_{\text{in}}), \delta_r(k, z_{\text{in}})$  at the desired initial redshift  $z_{\text{in}}$ .

$\delta_b(k, z_{\text{in}}), \delta_c(k, z_{\text{in}})$  are then trivial linear combinations of  $\delta_m, \delta_r$  and can be used as initial conditions for N-body codes or perturbative calculations. Only this particular matching is guaranteed to recover the correct linear evolution at low redshifts.

### Appendix B: Spherical collapse

In this appendix we provide more details on the spherical collapse calculation of Sec. IIB. Following the notation of App. A in [35], we replace  $t$  with  $\ln a$  as time coordinate and introduce

$$y_s(a) = \frac{R_s(a)}{R_{\text{in}}} - \frac{a}{a_{\text{in}}}, \quad s = c, b, \quad (\text{B1})$$

where the second term subtracts out the Hubble flow. This implies that  $y_s(a_{\text{in}}) = 0$  and

$$1 + \delta_s(a) = [1 + \delta_s(a_{\text{in}})] \left[ \frac{a_{\text{in}}}{a} y_s(a) + 1 \right]^{-3}. \quad (\text{B2})$$

We choose  $a_{\text{in}} = a_{\text{dec}} = 10^{-3}$ . Further, we have

$$\frac{R_b}{R_c} = \frac{y_b + a/a_{\text{in}}}{y_c + a/a_{\text{in}}}. \quad (\text{B3})$$

Denoting derivatives with respect to  $\ln a$  as primes, the equation for  $y_s$  then is (this is a generalization of Eq. (A9) in [35])

$$y_s'' + \frac{H'}{H} y_s' - \left( 1 + \frac{H'}{H} \right) y_s = -\frac{1}{2} \Omega_m(a) \left( \frac{a}{a_{\text{in}}} + y_s \right) G_s$$

$$G_s = \sum_{t=c,b} f_t \begin{cases} \delta_t, & R_t \leq R_s \\ \max\{0, (1 + \delta_t)(R_s/R_t)^3 - 1\}, & R_s < R_t \end{cases}. \quad (\text{B4})$$

The source term  $G_s$  is continuous, but not differentiable at  $R_b = R_c$ , where it reduces to  $G_b = G_c = \delta_m$ .

This means that the response of the tophat evolution to  $\theta_{bc}$  around  $\theta_{bc} = 0$  is ill-defined, since we attempt to take a derivative at precisely this point. For this reason, we perform a continuously differentiable cubic spline interpolation between the two branches in the interval  $1 \leq R_b/R_c \leq 1.1$  (we have verified that the upper end of the range has negligible impact on the results). This corresponds to slightly smoothing the tophat density profiles of the shells. Crucially, the interpolation matches the exact result at  $R_b = R_c$ , and so ensures that the evolution is correct at linear order.

We now derive the initial conditions. At  $a_{\text{in}}$  we wish to impose

$$\delta_c(a_{\text{in}}) = \delta_{c,\text{dec}}; \quad \delta_b(a_{\text{in}}) \Big|_{\theta_{bc}=0} = f_{\delta,\text{dec}} \delta_{c,\text{dec}}, \quad (\text{B5})$$

where we use linear theory for the initial conditions, and  $\delta_c$  is assumed to be in the growing mode. Our default choice is  $f_{\delta,\text{dec}} = 0$  (Sec. II B), but we allow for nonzero values here. Using that

$$\begin{aligned} \delta_{c,\text{dec}} &= A_+ D_+(\tau_{\text{dec}}) \\ \delta_{b,\text{dec}} - \delta_{c,\text{dec}} &= R_+ + \frac{\theta_{bc,0}}{H_0} D_r(\tau_{\text{dec}}) \end{aligned} \quad (\text{B6})$$

we can then trade the three mode amplitudes  $A_+$ ,  $R_+$ ,  $R_-$  for  $\delta_{c,\text{dec}}$ ,  $f_{\delta,\text{dec}}$ ,  $\theta_{cb,0}$  via

$$R_+ = \frac{f_{\delta,\text{dec}} - 1}{1 + (f_{\delta,\text{dec}} - 1)f_b} \delta_{c,\text{dec}}. \quad (\text{B7})$$

Note that even for  $f_{\delta,\text{dec}} = 1$  ( $R_+ = 0$ ),  $\delta_{b,\text{dec}} \neq \delta_{c,\text{dec}}$  due to the second term in Eq. (B6). Neglecting this term would lead to a spurious constant contribution to  $\delta_b - \delta_c$  which is proportional to  $(\theta_{bc}/aH)_{\text{dec}}$ . Finally, note that  $\theta_s = 3aH(H^{-1}\dot{R}_s/R_s - 1)$ . We thus have  $y'_s(a_{\text{in}}) = -\delta'_s(a_{\text{in}})/3$ . With these relations the initial conditions for the spherical collapse are completely specified in terms of  $\delta_{c,\text{dec}}$ ,  $f_{\delta,\text{dec}}$ ,  $\theta_{cb,0}$ .

Fig. 6 shows the resulting collapse threshold as a function of  $\theta_{bc,0}/H_0$ . The red filled triangles show the default case ( $f_{\delta,\text{dec}} = 0$ ), while the dotted line shows the result for an Einstein-de Sitter universe. Specifically, we set  $\Omega_m \rightarrow 1$  while adjusting  $\Omega_b$  to keep  $f_b$  at the same value as in the fiducial cosmology. Further, since the physically relevant quantity is  $(\theta_{bc}/aH)_{\text{dec}}$ , we plot the Einstein-de Sitter result as a function of  $\sqrt{\Omega_m}\theta_{bc,0}/H_0$ , where  $\Omega_m = 0.27$  is the fiducial value. We see that the effect of  $\theta_{bc}$  on  $\delta_{\text{crit}}$  is only very weakly dependent on cosmology. The green stars in Fig. 6 show the result obtained when forcing the same gravity to act on both shells, by setting  $R_b = R_c$  in the evaluation of  $G_s$  in Eq. (B4). This shows that our results are insensitive to the details of the spline interpolation used in the evaluation of Eq. (B4). Finally, the blue open triangles in Fig. 6 show the result for setting  $f_{\delta,\text{dec}} = 1$ . In this case, both matter components have the same overdensity initially and only differ via  $\dot{R}_b \neq \dot{R}_c$  (recall that both shells

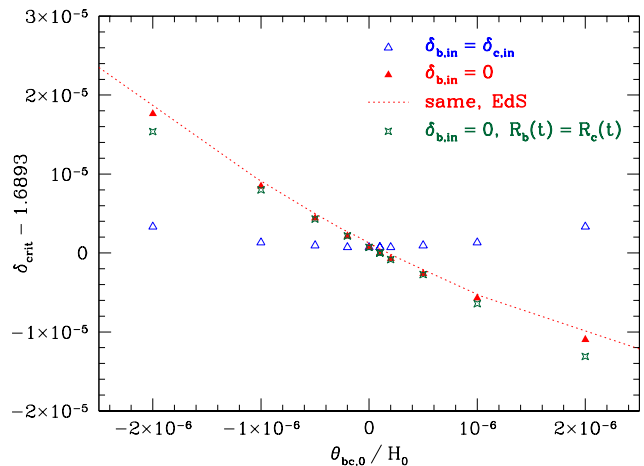


FIG. 6: Collapse threshold  $\delta_{\text{crit}}(z = 1.2)$  as a function of  $\theta_{bc,0}/H_0$  for different initial conditions and cosmologies (see text). The red filled triangles correspond to the default case discussed in Sec. II B.

always have the same initial radius). In this case,  $\theta_{bc} = 0$  corresponds approximately to a local minimum in  $\delta_{\text{crit}}$ . As argued in Sec. II B however, we expect  $f_{\delta,\text{dec}} = 0$  to be the physically relevant case.

In the previous preprint version of this paper, we reported a slope  $\partial\delta_{\text{crit}}/\partial(\theta_{bc,0}/H_0)$  that is roughly one order of magnitude higher than the value given here. That result is incorrect and affected by three issues. First, the previous implementation of initial conditions included a spurious contribution to  $R_+$  proportional to  $(\theta_{bc}/aH)_{\text{dec}}$  [see discussion after Eq. (B7)]. Second, different initial radii of the baryon and CDM shells were used, which results in an evolution that does not follow linear theory initially. Finally, the previous calculation used the non-differentiable force term in Eq. (B4), i.e. without spline interpolation, which further increases the slope (the different initial radii shift the discontinuity in the derivative  $\partial\delta_{\text{crit}}/\partial(\theta_{bc,0}/H_0)$  away from  $\theta_{bc,0} = 0$ ).

- 
- [1] D. J. Eisenstein, I. Zehavi, D. W. Hogg, R. Scoccimarro, M. R. Blanton, R. C. Nichol, R. Scranton, H.-J. Seo, M. Tegmark, Z. Zheng, et al., *Astrophys. J.* **633**, 560 (2005), astro-ph/0501171.
- [2] S. Cole, W. J. Percival, J. A. Peacock, P. Norberg, C. M. Baugh, C. S. Frenk, I. Baldry, J. Bland-Hawthorn, T. Bridges, R. Cannon, et al., *MNRAS* **362**, 505 (2005), astro-ph/0501174.
- [3] R. Barkana and A. Loeb, *MNRAS* **415**, 3113 (2011), 1009.1393.
- [4] D. Grin, O. Doré, and M. Kamionkowski, *Phys. Rev. D* **84**, 123003 (2011), 1107.5047.
- [5] M. T. Soumagnac, R. Barkana, C. G. Sabiu, A. Loeb, A. J. Ross, F. B. Abdalla, S. T. Balan, and O. Lahav, *ArXiv e-prints* (2016), 1602.01839.
- [6] M. Shoji and E. Komatsu, *Astrophys. J.* **700**, 705 (2009), 0903.2669.
- [7] G. Somogyi and R. E. Smith, *Phys. Rev. D* **81**, 023524 (2010), 0910.5220.
- [8] F. Bernardeau, N. Van de Rijdt, and F. Vernizzi, *Phys. Rev. D* **87**, 043530 (2013), 1209.3662.
- [9] D. Tseliakhovich and C. Hirata, *Phys. Rev. D* **82**, 083520 (2010), 1005.2416.
- [10] N. Dalal, U.-L. Pen, and U. Seljak, *JCAP* **11**, 007 (2010), 1009.4704.
- [11] J. Yoo, N. Dalal, and U. Seljak, *JCAP* **7**, 018 (2011), 1105.3732.
- [12] J. Yoo and U. Seljak, *Phys. Rev. D* **88**, 103520 (2013), 1308.1401.
- [13] Z. Slepian and D. J. Eisenstein, *MNRAS* **448**, 9 (2015), 1411.4052.
- [14] J. Blazek, J. E. McEwen, and C. M. Hirata, *ArXiv e-prints* (2015), 1510.03554.
- [15] P. McDonald, *Phys. Rev. D* **74**, 103512 (2006), arXiv:astro-ph/0609413.
- [16] V. Assassi, D. Baumann, D. Green, and M. Zaldarriaga, *JCAP* **8**, 056 (2014), 1402.5916.
- [17] M. Mirbabayi, F. Schmidt, and M. Zaldarriaga, *JCAP* **7**, 030 (2015), 1412.5169.
- [18] D. Baumann, A. Nicolis, L. Senatore, and M. Zaldarriaga, *JCAP* **7**, 051 (2012), 1004.2488.
- [19] L. Senatore (2014), 1406.7843.
- [20] K. Ahn, *ArXiv e-prints* (2016), 1603.09356.
- [21] D. Tseliakhovich, R. Barkana, and C. M. Hirata, *MNRAS* **418**, 906 (2011), 1012.2574.
- [22] E. Visbal, R. Barkana, A. Fialkov, D. Tseliakhovich, and C. M. Hirata, *Nature (London)* **487**, 70 (2012), 1201.1005.
- [23] C. Popa, S. Naoz, F. Marinacci, and M. Vogelsberger, *ArXiv e-prints* (2015), 1512.06862.
- [24] A. Lewis, A. Challinor, and A. Lasenby, *Astrophys. J.* **538**, 473 (2000), astro-ph/9911177.
- [25] V. Assassi, D. Baumann, and F. Schmidt, *JCAP* **12**, 043 (2015), 1510.03723.
- [26] J. R. Bond, S. Cole, G. Efstathiou, and N. Kaiser, *The Astrophysical Journal* **379**, 440 (1991).
- [27] S. Cole and N. Kaiser, *MNRAS* **237**, 1127 (1989).
- [28] H. J. Mo and S. D. M. White, *MNRAS* **282**, 347 (1996).
- [29] K. Ichiki and M. Takada, *Phys. Rev. D* **85**, 063521 (2012), 1108.4688.
- [30] F. Schmidt, W. Hu, and M. Lima, *Phys. Rev. D* **81**, 063005 (2010), 0911.5178.
- [31] M. Tellarini, A. Ross, G. Tasinato, and D. Wands, *JCAP* **1507**, 004 (2015), 1504.00324.
- [32] P. McDonald and A. Roy, *JCAP* **8**, 20 (2009), 0902.0991.
- [33] F. Bernardeau, S. Colombi, E. Gaztañaga, and R. Scoccimarro, *Phys. Rep.* **367**, 1 (2002), arXiv:astro-ph/0112551.
- [34] M. Lewandowski, A. Perko, and L. Senatore, *JCAP* **5**, 019 (2015), 1412.5049.
- [35] F. Schmidt, M. V. Lima, H. Oyaizu, and W. Hu, *Phys. Rev. D* **79**, 083518 (2009), 0812.0545.